electricity

MDPI

Article

Energy Management Strategy for Hybrid Electric Vehicles Based on Adaptive Equivalent Ratio-Model Predictive Control

Farah Mahdi Ali * and Nizar Hadi Abbas

Department of Electrical Engineering, University of Baghdad, Baghdad 10071, Iraq; dr.nizar.hadi@coeng.uobaghdad.edu.iq
* Correspondence: farah.m.ali@coeng.uobaghdad.edu.iq

Abstract: The research and development of hybrid electric vehicles has become a significant goal for large automotive manufacturers. The hybrid electric vehicle integrates a conventional engine and one or more electric motors powered by a battery, offering better fuel economy and lowering exhaust emissions. This paper develops an optimal energy management algorithm based on Model Predictive Control that can produce optimal control parameters for power distribution between the battery unit and generator. The energy management strategy adapts this optimal power distribution by adjusting the objective function equivalent parameter of the controller according to changes in driving conditions. Dynamic programming is utilized offline to find the reference state of charge of the battery and used as the reference trajectory of our proposed strategy. Simulation results using different driving cycles show that the proposed method has better power distribution compared with two other strategies. The final state of charge reached a higher level, and the energy-saving percentage rose compared to the conventional algorithm.

Keywords: hybrid electric vehicle; vehicle dynamics; energy management strategy; model predictive control

Citation: Ali, F.M.; Abbas, N.H. Energy Management Strategy for Hybrid Electric Vehicles Based on Adaptive Equivalent Ratio-Model Predictive Control. *Electricity* **2024**, *5*, 972–990. https://doi.org/10.3390/electricity5040049

Academic Editor: Andreas Sumper

Received: 31 October 2024
Revised: 20 November 2024
Accepted: 25 November 2024
Published: 3 December 2024

1. Introduction

The development of the automotive industry has been obstructed by the problem of energy depletion and environmental pollution [1]. In 2022, the Fit for 55 package was passed by the European Parliament. It will impose a limitation on the 2030 CO_2 emissions targets for passenger cars and light-duty vehicles, respectively, from −31% to −50% and from −37.5% to −55%, relative to 1990 levels [2]. So, battery electric vehicles (BEVs) and hybrid electric vehicles (HEVs) with environmental protection began to gain more attention. Though BEVs produce no tailpipe emissions (environmentally friendly) and generally need less maintenance than conventional internal combustion engine (ICE) vehicles, they suffer from several issues relating to limited driving range, inadequate infrastructure, and battery shortcomings such as low power density and high cost. As such, hybrid electric vehicles are a critical solution in the adoption of fully BEVs. Hybridizing technologies have recently been employed in both passenger and heavy-duty vehicles [3].

Having two power sources in HEVs presents a problem: how much of this power should be distributed to each source throughout the journey? This problem is known as energy management strategies (EMS). EMS for HEVs seek to maximize the efficiency of the hybrid powertrain and minimize the fuel consumption of the engine. Energy distribution of the engine, motor and generator needs to be coordinated so that the engine can operate in the low-energy and high-efficiency areas and recover sufficient energy by the regenerative braking of the motor [4].

Various strategies are proposed to solve this problem and are generally grouped into two categories: the rule-based (RB) control strategy and the optimization-based (OB) control strategy. The RB energy management strategy employs the use of predefined rules

based on the current state of the operation and relies on a large amount of engineering experience analysis [5]. Optimization-based control strategies include an objective function with constraints to be maximized or minimized and obtain a noncausal solution, which mainly comprises real-time instantaneous optimization and global optimization [6]. A third category also exists, which is a Learning-Based (LB) EMS. LB uses sophisticated data mining techniques to extract optimal control rules from vast historical and real-time data [3], for example, reinforcement learning [6] and neural network learning.

The design of the EMS for HEVs for both strategies was widely investigated in the literature. Several Rule-Based (RB) strategies exist. For example, [7] presents a simple RB EMS to select the optimal driving mode. The control design variable is the maximum power level of the HEV during pure electric driving mode. The proposed method requires much less computation time compared with dynamic programming (with the same accuracy). In addition, the average fuel saving for the proposed method is improved. Another work in [8] presents an Adaptive Rule-Based Energy Management Strategy (ARBS EMS) for HEVs, which can be implemented on-line to optimize fuel consumption without prior knowledge of the drive cycle or the engine efficiency map. As a result, the proposed method is particularly suitable for aftermarket hybridization.

On the other hand, the Equivalent Cost Minimization Strategy (ECMS), as one of the optimization-based strategies is adopted in the EMS. It can obtain a near-optimal solution with low computational burden. In [9], a blend of rule-based energy management strategy and ECMS is designed as an EMS for the application of Electrical Variable Transmission (EVT) in a passenger HEV. Their work provided appropriate energy management, fulfilled the required objectives and was capable of minimizing fuel consumption.

Another optimization-based method commonly used is the Pontryagin's Minimum Principle (PMP). This method is flexible and has less computational effort. Ref. [10] applied PMP to compute the optimal EMS offline, then a comparison with an on-line rule-based management strategy is done. They also established the Pareto optimal front between the two state variables used in the objective function: battery RMS current and fuel usage.

Dynamic Programming (DP) strategy has been used to guarantee globally optimal solutions and applied with various goals of cost formulation such as minimizing fuel or energy consumption. However, DP strategies are typically used as an offline method for computing the global optimum and are rarely appropriate in real-time applications [11]. Though both PMP and DP solve offline optimization problems, DP has better robustness and is able to manage state variable limitations as required [12]. In addition, DP algorithms can be executed if detailed information on a driving cycle is available [13].

Model Predictive Control (MPC) is an optimization-based finite-time feedback control scheme based on the iterative solution of a specific problem at every sampling instant to find control inputs [14].

Although classic control suits a considerable percentage of all control problems perfectly, MPC is a suitable method for nearly all problems, including those with feasibility issues and a lack of control theoretical knowledge. Unlike conventional control approaches, which employ precomputed control laws, MPC uses both anticipation and optimization to evaluate the control signal [15].

Also, Model Predictive Control (MPC) is used widely as an optimization-based EMS strategy. As a predictive controller, MPC is perfect to use, especially with its good ability to manage multiple variables and constraints in control problems. This strategy can compute the required control action in a predefined horizon window at each sampling moment to provide an optimal real-time solution [16].

A hybrid energy storage system (HESS) for the HEV composed of ultracapacitor (UC) and battery units is introduced in [17]. They proposed a multi-objective optimization EMS based on velocity prediction using a generalized regression neural network (GRNN). Then, the dual-mode power-split HEV power distribution is handled by MPC as a rolling optimization problem in its prediction horizon. Two objectives are considered in the cost function: fuel economy and battery protection. Compared with several other strategies,

the proposed method offered less fuel consumption and reduced the root mean square (RMS) of battery current. In [9], an explicit nonlinear model predictive control (eNMPC) approach such as EMS for a plug-in HEV is developed based on an Autonomie high-fidelity model of the powertrain within a dSPACE HIL platform. The control-oriented model was utilized by the explicit NMPC method to determine the optimized control inputs within an offline procedure. First, the cost function was minimized according to the constraints; then, an on-line procedure is activated using these results. The proposed scheme reduced fuel consumption and preserved real-time capability and drivability indices.

In most published papers, typically, the general-purpose convex optimization software (for example, CVX) has been used to resolve the optimization problem [18]. However, in [18], an investigation for resolving a convex formulation of the MPC optimization problem with nonlinear losses is introduced. By using the projected interior-point method, the computational requirements have been reduced significantly. Ref. [16] proposes an improved model predictive control framework that enhances the EMS by integrating vehicle-to-vehicle (V2V) and vehicle-to-infrastructure (V2I) communication. First, it utilized the Particle Swarm Optimization (PSO) technique to improve speed prediction accuracy, particularly when the vehicle is traveling between traffic intersections. V2V is used to find an instantaneous safe speed, which helps update predicted speeds. Then, the optimal speed sequence is planned in advance when approaching traffic intersections. The combination of speed prediction, speed planning, and rolling optimization leads to an effective MPC-based optimal energy management strategy, resulting in a reduction in fuel consumption compared to traditional rule-based strategies. A Hybrid energy storage system (HESS) composed of a supercapacitor and battery for EV is considered in [19]. Driving cycle prediction is made under the framework of the MPC algorithm using a long short-term memory-based method. Three strategies, including fuzzy, DP and MPC, are evaluated and compared. The results show that the MPC method lessens the stress on the battery in the HESS and significantly reduces energy dissipation. In [20], the focus is on optimizing the prediction time horizon to enhance the adaptability of the EMS to variable driving conditions. Using a Radial Basis Function (RBF) neural network to predict future vehicle velocity, an Adaptive Network-Based Fuzzy Inference System (ANFIS) system dynamically adjusts the time horizon based on historical driving data. The calculation time and the fuel consumption are reduced compared to traditional fixed-horizon MPC strategies. Another research study that aims to reduce the computational time, making it suitable for online applications, is introduced in [21]. They present a stochastic MPC method enhanced by reinforcement learning for optimizing energy management in plug-in hybrid electric vehicles. The strategy involves training a reinforcement learning controller using the Q-learning algorithm to optimize power distribution across different driving cycles. The reinforcement learning controller is integrated into the MPC framework to determine the optimal battery power in real-time.

Most studies optimize the MPC based on the vehicle dynamics and standard drive cycles. However, considering the driving condition of the road and the information about real-world traffic environment will have a significant impact on the performance of MPC-based EMS.

Motivated by this, in this paper, DP is first used offline to find optimal SOC by integrating API Google map information about the road. This optimal solution is considered as a reference trajectory to be followed by the proposed enhanced MPC strategy as an on-line EMS. Next, the equivalence parameter of the MPC objective function is adjusted (in real-time) to adapt to changes due to driving behavior and according to current driving conditions. This adjustment guarantees charge sustainability and is applied in the EMS control level rather than applied in the prediction level. Finally, the energy consumption (EC) superiority of the proposed method over the rule-based CD-CS and original MPC algorithms is proven.

2. Materials and Methods

2.1. Hybrid Electric Vehicle Model Description

The Hybrid electric vehicles can be generally categorized into three types [22].

2.1.1. Series Hybrid Electric Vehicles

This system has a battery pack, an electric generator, a decoupled-from-wheel engine, and a motor.

2.1.2. Parallel Hybrid Electric Vehicles

In a parallel HEV power system, both the electric motor and ICE can run simultaneously to rotate the wheels since they are mechanically connected to the transmission system.

2.1.3. Series-Parallel Hybrid Electric Vehicles

This configuration gains all the advantages of series and parallel modes, such as fuel economy improvement and extended travelling mileage. The three configurations are shown in Figure 1.

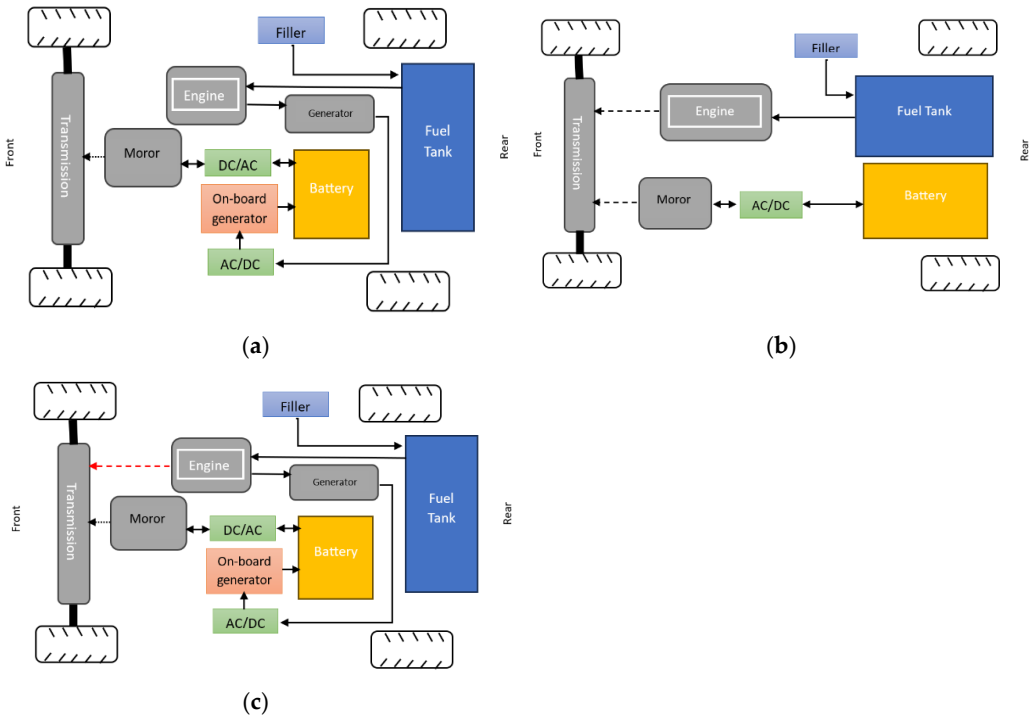

Figure 1. HEV Schematic diagram: (**a**) series (**b**) parallel (**c**) series-parallel.

To increase the range of HEVs, Plug-In Hybrid Electric Vehicles (PHEVs) were also developed. They are similar to HEVs with the feature that the utility grid can be used to charge the battery.

The vehicle considered for this study was built in [23] and is called an Extended Range Electric Vehicle (EREV). It has a secondary on-board auxiliary power unit (APU), which consists of an ICE with a paired generator. An EREV is often equipped with a larger battery compared to other HEVs, which allows for more pure electrical range [24]. Although series plug-in HEVs can be considered as a type of EREV, there are differences regarding the powertrain design, the ICE configuration, and the size of the battery unit [25]. See Figure 2.

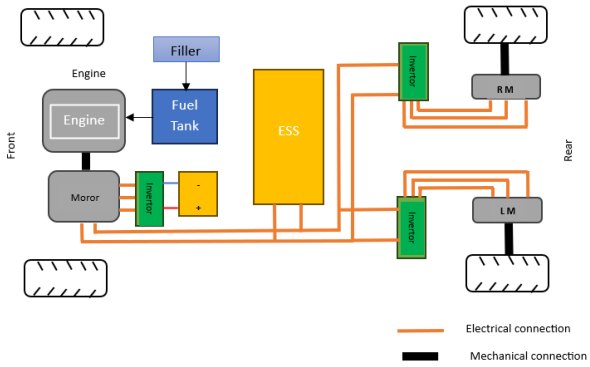

Figure 2. Schematic diagram of the EREV powertrain.

Indeed, each type of HEV has unique EMS requirements. The control strategy proposed for an EREV would focus more on managing the generator and battery interactions. But it can be adapted to other types of Hybrid Electric Vehicles with some key considerations:

1. For parallel HEVs where both engine and electric motor can drive the wheels, the algorithm is more complex and there is a need to adjust the control strategy to include a power-split between both of them.
2. The Series-Parallel (Power-Split) HEV, which combines the features of both series and parallel hybrids, would require an even more sophisticated model to optimize both power split and SOC management simultaneously. So, an adjustment to the algorithm formulation is also needed to handle the increased complexity.
3. For Mild Hybrids, which are typically parallel hybrids with a small electric motor that assists the ICE, the proposed EMS might need simplification since it focuses on optimizing when to use the electric assist to save fuel and the generator system may not be so prominent as in other architectures.
4. For the Plug-In Hybrid Electric Vehicle, which has larger batteries that can be charged externally, allowing for more electric-only driving, the proposed strategy is applicable after taking the "when to charge from the grid?" scenario into consideration.

2.2. Model of the Vehicle

Regarding the physical causality principles, the HEV modelling can adopt two approaches: the backward- and forward-facing modelling. In the backward scheme, the vehicle speed is assumed to be known, and the power request is computed using the drivetrain's kinematical relationships (simple and low computations). On the other hand, the forward scheme takes the driver commands as input and generates the vehicle's performance as output (complicated and high computations) [26]. The backward-facing modelling is adopted in this work. The model consists of a motorcycle engine directly coupled to a synchronous motor-generator unit (MG), an energy storage system (ESS), two independent motors (axial flux permanent magnet motors) for each rear wheel, and an inverter converter module to convert the 3-phase current generated into direct current (Figure 1). Table 1 listed the main parameters of the vehicle.

Table 1. Definition of EREV parameters.

EREV Parameters	Value
Engine Max. Power	80.7 (kW)
Engine Max. Torque	80 (Nm)
MG Max. Power (Peak)	83.8 (kW)
MG max torque (Peak)	200 (Nm)
Traction Motor Max. Power (Peak)	230 (kW)
Traction Motor Max. Torque (Peak)	500 (Nm)

Table 1. *Cont.*

EREV Parameters	Value
ESS Max. Capacity	18.9 (kWh)
ESS Nominal Pack Voltage	340 (V)
ESS Discharge Power Limit (Peak)	208 (kW)
ESS Charge Power Limit (Peak)	102 (kW)

The engine for an EREV does not have to run in wide speed ranges, which makes it operate in a high-efficiency area. As a result, the noise and vibration can be reduced further [25].

2.2.1. Engine Model

A variety of methods exist for ICE modelling techniques with varying levels of detail. The modelling can focus on the high level including only parameters of concern in the model. Maps were calibrated for the purpose of engine modelling. See Figure 3.

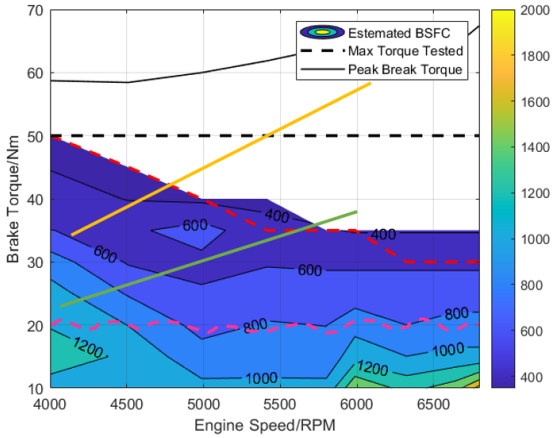

Figure 3. The BSFC map for the engine with an approximated behavior of different driving traces.

The fuel consumption of the engine is measured by the fuel mass flow rate $\dot{m}_f$ and is given by the nonlinear function of engine torque and engine speed:

$$\dot{m}_f = f_e(\omega_e, T_e) \tag{1}$$

where ω_e and T_e are the engine rotational speed and torque, respectively. The actual fuel consumption of the whole driving cycle (FC_{act}) can be calculated from the following equation:

$$FC_{act} = \int_{t_f}^{t_0} f_e(\omega_e, T_e)dt \tag{2}$$

The estimated brake-specific fuel consumption (BSFC) map for the engine (VFR800 engine) is based on a map used by [23]. It is pictured in Figure 3. The BSFC map helps in estimating $\dot{m}_f$ at the selected generator operation setpoint. Equation (3) determines $\dot{m}_f$ using the BSFC map.

$$\dot{m}_f = BSFC \times P_{gen} \times \frac{1}{3600} \tag{3}$$

The engine speed and load torque limits were [4000–7000] RPM and [0, 50] Nm, respectively. The map shows that BSFC decreases with low speed and high torque. Thus, to reduce the fuel consumption rate, the system must operate near low speed and high torque regions. The BSFC map is a fixed characteristic of the engine; however, the driving strategies can influence how the efficiently the engine and reduce the fuel consumption. An estimation to three different driving strategies can be added:

1. Eco-driving (pink dotted line) remains in the lower BSFC regions, indicating better fuel efficiency.
2. City driving (green line) fluctuates within the mid-range BSFC zones due to stop-and-go behavior.
3. Aggressive driving (orange line) extends into higher torque and RPM areas, resulting in less efficient fuel usage.

2.2.2. Propulsion System Model

The propulsion system consists of two motors attached to the rear wheels. The efficiency map for the motor and gearbox combined components is shown in Figure 4. The black dotted lines indicate the motor's maximum torque and the contours of different colors indicate the efficiency of the motor in various working areas.

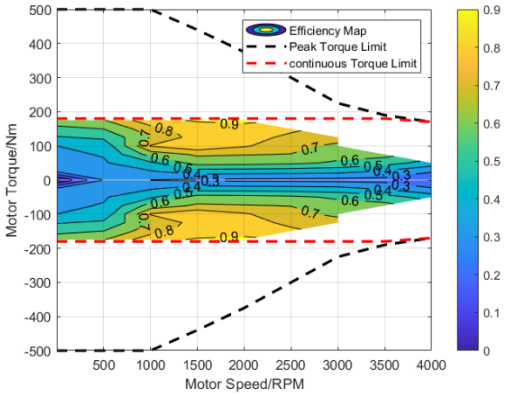

Figure 4. Propulsion system Efficiency map.

2.2.3. Vehicle Road-Load Model

A longitudinal vehicle model is created using the road load equation to compute the amount of demanded power by the vehicle (P_{dem}) [27]. See Figure 5.

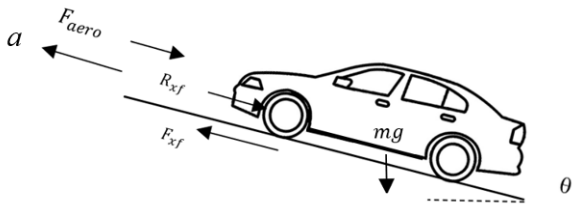

Figure 5. The forces exerted on the vehicle.

The mathematical relationships for all the forces exerted on the vehicle are provided in Equations (4) and (5):

$$F_x = m\,\mathrm{a} + F_{aero} + R_x \pm F_g F_{aero} = \frac{\rho}{2} A C_d v^2, R_x = mgC_r\cos(\theta), F_g = mg\sin(\theta) \quad (4)$$

$$P_{dem} = F_x \times v \quad (5)$$

2.2.4. Motor Model

The required motor torque is determined by applying the traction force values to the traction motor model. As F_x is for both motors, a single motor torque is equal to half split between the wheels.

Thus, the single motor torque is computed as Equation (6):

$$T_{mot}{}^{req} = \frac{1}{2} F_x R_w \left(\frac{1}{R_{gear}}\right) \quad (6)$$

$$P_{elec}{}^{req} = T_{mot}{}^{req}\omega_{mot}\left(\frac{1}{\eta_{mot}\eta_{gear}}\right) \tag{7}$$

The motor's torque ($T_{mot}{}^{req}$) is used to obtain the net propulsion power demand ($P_{elec}{}^{req}$) in Equation (7). The auxiliary power demand (P_{aux}) from accessory electrical components is considered too. The efficiency of the motor is a look-up function of its speed ω_{mot} and torque T_{mot} (see Figure 4). The final net power demand from ESS (P_T^{ess}) is obtained as in Equation (8)

$$P_T^{ess} = P_{elec}{}^{req} + P_{aux} \tag{8}$$

All parameters are defined in Table 2.

Table 2. Parameters definition for the HEV model.

Term	Definition
m	mass of the vehicle without passengers (1875 kg)
a	acceleration/deceleration of the vehicle
F_x	longitudinal traction force
F_{aero}	longitudinal aerodynamic drag force
P_{dem}	Power demand
R_x	rolling resistance force
F_g	Gravitational force
g	Gravity coefficient (9.81 m/s^2)
ρ	The mass density of the air (1.225 kg/m^3)
A	frontal area (0.4 m^2)
C_d	aerodynamic resistance coefficient (0.34)
v	speed of the vehicle (m/s)
C_r	rolling resistance coefficient
R_w	Effective radius of the wheel (0.346 m)
η_{gear}	efficiency of planetary gear System (90%)
η_{mot}	efficiency of the motor
ω_{mot}	Motor speed
R_{gear}	Gear ratio (4.2)

2.2.5. Battery Model

Equivalent circuit modelling is typically used in battery modelling. A controlled voltage source connected in series with a constant resistance is used to model the Lithium-Ion (Li-Ion) battery [28]. The model, which is called the zeroth order equivalent circuit, is represented by the Equation (9):

$$V_{batt} = U_{batt} - I_{batt}{\cdot}R_0 \tag{9}$$

where U_{batt} is No-load battery voltage, R_0 is internal resistance, I_{batt} is battery current and V_{batt} is the battery voltage.

A more accurate model is used in the literature and represented by Equation (10), where the voltage of the battery is given by:

$$V_{batt} = U_{batt} - I_{batt}{\cdot}R_0 - \sum_{1}^{Np} V_N \tag{10}$$

Np is the number of resistor-capacitor (RC) pairs, V_N is the voltage of the nth RC pair.

In this paper, a better model (a dual polarization battery model), which has two RC pairs, as shown in Figure 6, is used.

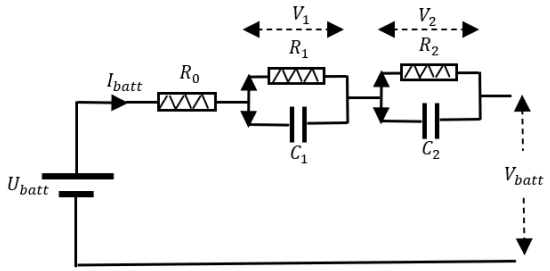

Figure 6. The diagram of a dual polarization battery model.

The resistance and capacitance (R_1, R_2, C_1, and C_2), which represents electrochemical and concentration polarization, may track transient behavior during charge and discharge cycles. This model is more accurate than a simple resistor [29]. Adding more RC pairs in the circuit model causes complexity to rise without improving the accuracy of the model; therefore, models beyond the second order are generally not used [30]. The battery model is represented as per Equation (10): open-circuit voltage, the internal resistance of the battery, and the resistance and capacitance values adopted based on empirical data. See Table 3. This model is used in battery management systems for predicting battery behavior during charging and discharging cycles. The function of each module is as follows:

Table 3. Dual polarization battery parameters definition.

Parameter	Definition
V_{batt}	DC battery voltage (V)
U_{batt}	No load battery voltage (V)
R_0	Internal resistance (Ω)
I_{batt}	Battery current (A)
V_1	Voltage across the first RC branch (V)
V_2	Voltage across the second RC branch (V)
Q_{max}	Maximum battery capacity (Ah)

(U_{batt}), the open-circuit voltage of the battery. This is the theoretical voltage of the battery when no load is connected.

(R_0), the internal resistance causes an instantaneous voltage drop proportional to the current drawn (I_{batt}). This drop affects the efficiency of the battery.

First RC Network (R_1, C_1): Represents the fast transient response of the battery. When there are sudden changes in load, the voltage across this RC network adjusts quickly, capturing the immediate voltage recovery effects.

Second RC Network (R_2,C_2): Models the slow transient response and long-term relaxation effects in the battery. This RC network represents how the battery voltage recovers slowly after being under load for an extended period. Using both (R1–C1 and R2–C2) allows the model to capture both short-term and long-term dynamics, making it more accurate than simpler models.

(V_{batt}) Terminal Voltage: Represents the actual voltage measured at the battery terminals after accounting for all internal losses and transient effects.

The ratio of the battery's remaining power to its overall capacity is known as the state of charge (SOC). The battery's limited charging capability is represented in the battery charging power limitation and SOC limitation. The charging capacity of the battery is limited, which is reflected in SOC limitation and battery charging power limitation. It can be obtained as an integral of the current and related to the overall battery current capacity.

$$SOC = -\frac{1}{Q_{max}} \int_0^t I_{batt} dt \tag{11}$$

$$\frac{\Delta SOC}{\Delta k} = \frac{SOC(k) - SOC(k-1)}{\Delta k} = -\frac{I_{batt}(k)}{Q_{max}} \tag{12}$$

Moreover, battery ageing can be accelerated by frequent charging and discharging processes.

2.3. Regenerative Braking Control

A combined motor-generator (MG) unit, used in most HEVs, is utilized to provide regenerative braking. During regenerative braking, the motor converts mechanical energy into electrical energy. Because of regenerative braking, the mechanical brakes last longer since they are used much less. To avoid overcharging the battery from regenerative braking, the charging process must be stopped when SOC reaches a particular threshold value. The maximum charging power cannot be exceeded by the battery side regenerative braking power. Otherwise, the battery is damaged. The regenerative braking algorithm, which computes the required mechanical brake power and the battery power, is described in Algorithm 1, where $P_{max}^{mot\_reg}$ is the maximum motor regenerative power, P_{Batt} is the power of the battery pack, and $P_{MechBrk}$ is the power generated by the mechanical brakes.

Algorithm 1: Regenerative Braking Algorithm

Input: P_T^{ess}, $P_{max}^{mot\_reg}$, SOC
Output: P_{Batt}, $P_{MechBrk}$
while $P_T^{ess} < 0$ **do**
  if $SOC \leq 9.5$ **then**
    if $P_T^{ess} \geq P_{max}^{mot\_reg}$ **then**
      $P_{Batt} = P_T^{ess}$
      $P_{MechBrk} = 0$
    else if $P_T^{ess} < P_{max}^{mot\_reg}$ **then**
      $P_{Batt} = P_{max}^{mot\_reg}$
      $P_{MechBrk} = P_T^{ess} - P_{max}^{mot\_reg}$

    else if $SOC > 9.5$ **then**
      $P_{Batt} = 0$
      $P_{MechBrk} = P_T^{ess}$

end

2.4. Trip Planner

MPC is considered an optimization-based strategy employed for the energy management problem. However, the performance of the MPC is sensitive to the model quality. A model mismatch, such as road conditions, weather, and sensor precision, affects the results obtained by the algorithm. Thus, extra information is used with the MPC to improve the prediction results [4]. Advancements in GPS, GIS, and Intelligent Vehicle Technologies, such as Vehicle-to-Vehicle (V2V) and Vehicle-to-Infrastructure (V2I) Communication Systems, have been employed to predict future driving conditions and improve the performance of MPC controllers. All these technologies can predict future driving conditions and enable the MPC to adapt its cost function or extend its prediction horizon accordingly. Therefore, Directions API, which is one of the services offered by Google Maps Platform, is used to obtain the average speed trace for the driving cycle based on the origin and destination locations inputs. So, in our case, using the Google Maps Directions API helps in obtaining speed traces that reflect current traffic conditions, making the driving cycle more realistic, thus allowing for more efficient proactive energy management. In this paper, speed trajectories were evaluated for two locations as follows:

1. Abu Dhabi (RM 1): the speed trace is considered for the origin and destination between two longitude and latitude coordinates points: [54.3775, 24.4541] and [54.5629, 24.3653], as shown in Figure 7.
2. Jordan (RM 2): the speed trace is considered between two longitude and latitude coordinates points: [35.8697, 32.0156] and [35.8976, 31.9678], as shown in Figure 8.

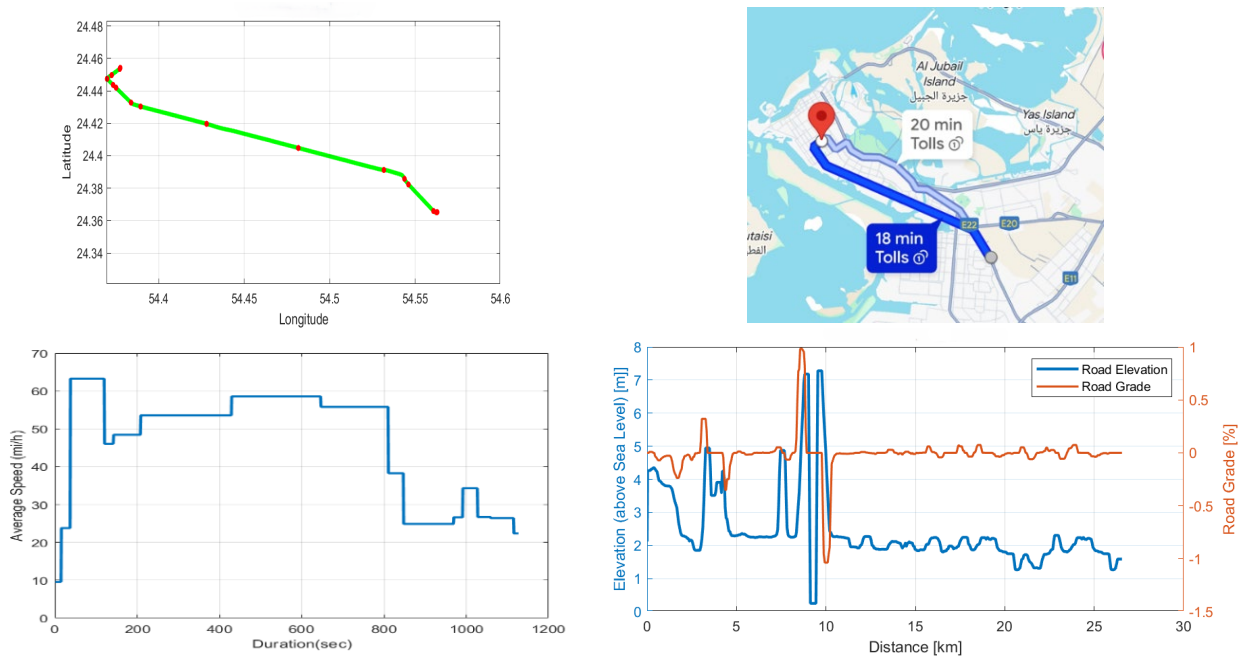

Figure 7. Road map 1 (RM 1).

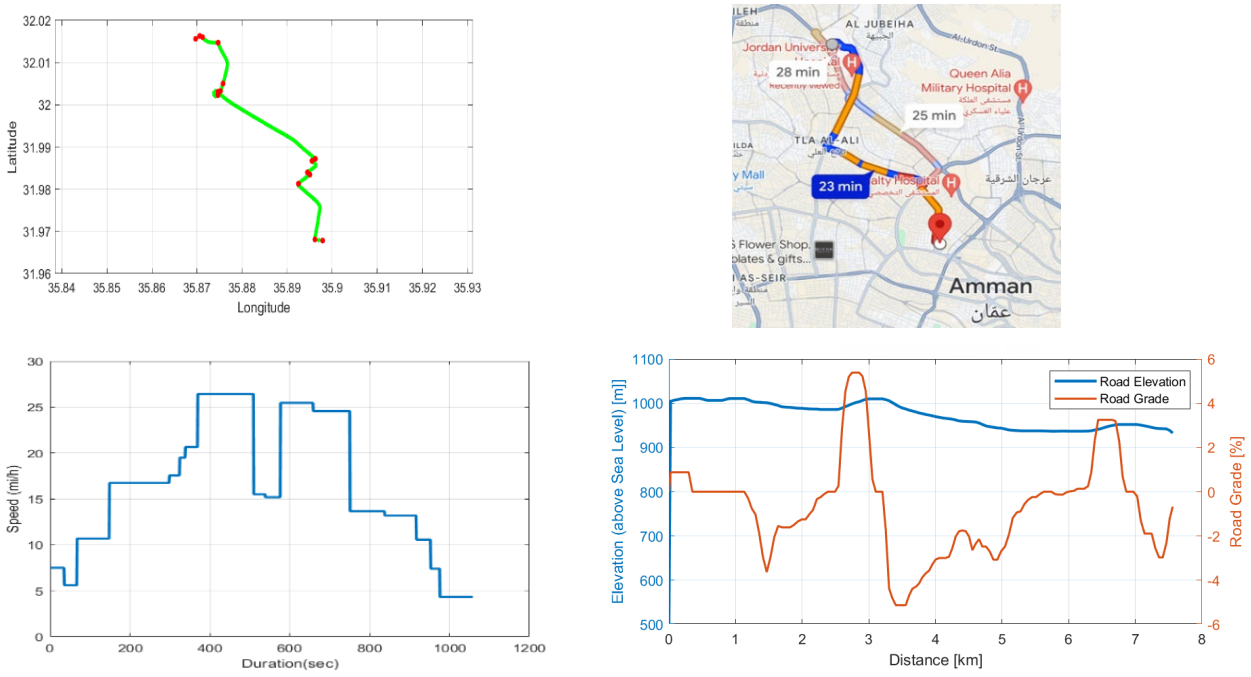

Figure 8. Road map 2 (RM 2).

2.5. Energy Management Strategy Modelling

After introducing the vehicle's model, an enhanced MPC method is developed to find two optimal inputs (SOC and P_{gen}) based on the objectives and constraints. However, the optimal SOC trajectory is first calculated within an offline procedure based on DP. Secondly, an on-line procedure is implemented using these results. The structure of the MPC-based EMS is illustrated in Figure 9.

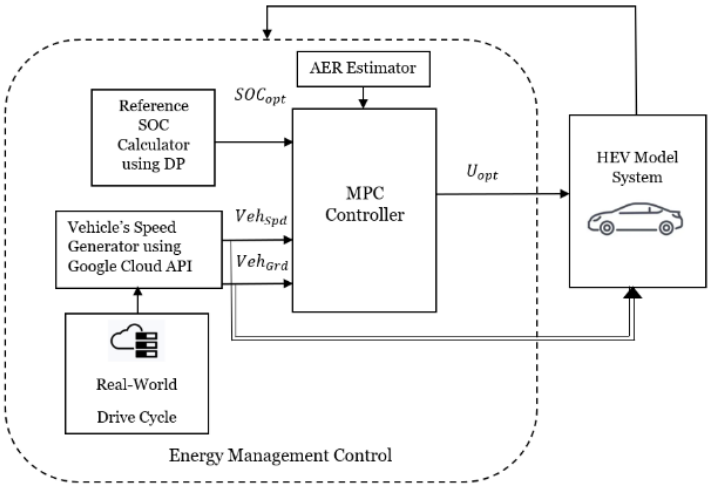

Figure 9. The structure of MPC-based EMS.

2.5.1. Dynamic Programming

Dynamic programming, developed by Richard Bellman, is a common method for EMS. Here, it was used to obtain the optimal SOC (SOC^*) to be used for the lower layer controller. DP simplifies a large problem by breaking it down into sub-problems and solving it recursively in an application of Bellman's principle of optimality. Consider a system described by the following:

$$x_{k+1} = f_k(x_k, u_k)$$

where x represents the state variable and u the control variable.

Despite DP generally proceeding backwards in time, it can be implemented in a forward propagation sense. Thus, the process started at the zeroth stage ($k = 0$) and traversed forwards. Then, the optimal control problem is to find the control sequences to minimize the cost function (J_k^*) (called the Hamilton-Jacobi-Bellman equation) in discrete time as shown in Equation (13):

$$\begin{gathered} J_k{}^*(SOC_k) = \min_{P_{fuel}, P_{ESS}} \{\hat{f}(SOC_k(P_{fuel_k}, P_{ESSk})) \\ + J_{k-1}{}^*(\hat{g}(SOC_k(P_{fuel_k}, P_{ESSk}))\} \\ \forall k : 0 \le k \le n-1 \\ s.t \\ SOC_{min} \le SOC_k \le SOC_{max} \\ P_{Battchg} \le P_{Batt} \le P_{Battdschg} \end{gathered} \tag{13}$$

where SOC_k, P_{fuel_k} and P_{ESSk} are the state and control variables corresponding to stage k, respectively. Here $\hat{f}$ (discrete approximations to f) represents the cost of moving from stage $k-1$ to k and $\hat{g}$ (discrete approximations to g) stands for the net cost up to stage $k-1$. Also, an extra condition, as in [23], is added to achieve a Distance to Empty (DTE) greater than or equal to the target distance.

2.5.2. EMS Based on AER-MPC

The goal of energy management is to reduce energy consumption throughout a given driving cycle using MPC. The optimization is carried out on the cost function J.

$$J = (\alpha \cdot \dot{m}_f)^2 + F_{eq}(\beta \cdot \Delta\, SOC)^2 \tag{14}$$

where α and β are weights applied to the input variables, $\Delta\, SOC$ is the difference between the actual and optimal SOC and F_{eq} represents the equivalence factor and plays an essential

role in energy consumption optimization [24]. F_{eq} is not necessarily a constant and could be varied with time. Some researchers consider this factor as a penalty and use either a constant value or take it as one of two:

$$F_{eq} = \begin{cases} 0 & for\ \ SOC_{act} = SOC_{opt} \\ \infty & otherwise \end{cases} \tag{15}$$

To improve the controller performance, F_{eq} is taken as a function of SOC and written as $F_{eq} = F_{eq}(SOC)$. Its value is adapted according to the current SOC status to prevent a high deviation from its target value and evaluated on-line in a separate procedure block called Adapted Equivalent Ratio (AER) estimator (See Figure 8). Thus, ensuring the SOC sustainability and better performance.

F_{eq} is discretized into S points:

$$\begin{gathered} F_{eq\_t} = F_{eq_{LL}} + \Delta F_{eq} \cdot t \quad t \in \{0, 1, \ldots, S\} \\ F_{eq_{LL}} \leq F_{eq\_t} \leq F_{eq_{UL}} \\ \Delta F_{eq} = f(\Delta SOC) \end{gathered} \tag{16}$$

$F_{eq_{LL}}$ and $F_{eq_{UL}}$ are the upper and lower boundaries of the equivalence ratio F_{eq}. Their values were heuristically determined and equal to 1×10^4 and 1×10^7, respectively. ΔF_{eq} is evaluated using reference SOC and a feedback signal from actual battery SOC.

Since $\dot{m}_f$ is a function of the generator output power (see Equation (3)), P_{gen} is considered as a control input. Then, the cost function over the horizon window becomes:

$$\arg \min_{SOC,\ P_{gen}} J = \sum_{k=0}^{N-1} \left(\alpha \cdot P_{gen}^{t+k}\right)^2 + F_{eq}\left(SOC^{t+k}\right) \cdot \left(\beta \cdot\ \Delta\ SOC^{t+k}\right)^2 \tag{17}$$

s.t.

$$\begin{gathered} 0\ \leq P_{gen}^{t+k}\ \leq {P_{gen}}^{max} \\ \hat{SOC}_{min}^{t+k} \leq SOC^{t+k} \leq \hat{SOC}_{max}^{t+k} \\ \overline{T}_{EM} \leq T_{EM} \leq \underline{T}_{EM} \end{gathered}$$

where SOC and P_{gen} are considered as the state and the control variables, respectively. N is the receding horizon. Actuator limitations (ICE, generator and EM) and battery SOC are the main constraints in the EMS–MPC problem.

3. Results

The performance of the proposed controller is validated by testing different drive traces.

3.1. The Standard Drive Cycle Results

Three standard driving cycles that simulate various power demands were implemented. They are commonly used in automotive testing to simulate real-world driving conditions.

(a) Urban Dynamometer Driving Schedule (UDDS): Data Source: it is defined by the Environmental Protection Agency (EPA) in the United States. It is often used to measure emissions and fuel economy in light-duty vehicles. It is designed to simulate city driving, including stop-and-go traffic.

(b) Highway Fuel Economy Test (HWFET): Data Source: The HWFET: it is also established by the EPA and is used for assessing highway fuel economy. It represents highway driving with a focus on steady-state cruising, higher speeds, and fewer stops (relatively constant speeds with minimal stops).

(c) UDDS-HWFET: the combined two cycles create a mixed driving profile that captures both urban (stop-and-go) and highway (steady cruising) conditions. Thus, it provides a more comprehensive evaluation of a vehicle's performance and energy efficiency across diverse real-world scenarios. First, the UDDS (Urban Dynamometer Driving

Schedule) indicates driving conditions in cities. Second, the HWFET (Highway Fuel Economy Driving Schedule) indicates driving conditions on highways. Finally, the two driving cycles are combined to simulate both driving conditions. The length of a single UDDS, HWFET, and combined driving cycle were 12 km, 16.5 km, and 28.5 km, respectively. The driving cycle was repeated multiple times (five times) in order to create a simulation drive cycle with a long distance, resulting in different driving distances (60 km, 82.5 km, and 142.5 km), as shown in Figure 10. The initial SOC was 90%. The road grade was zero for all traces. The original MPC and the conventional Charge Depletion/Charge Sustaining (CD/CS) strategies were also applied for comparison. The simulation results are shown in Figure 11.

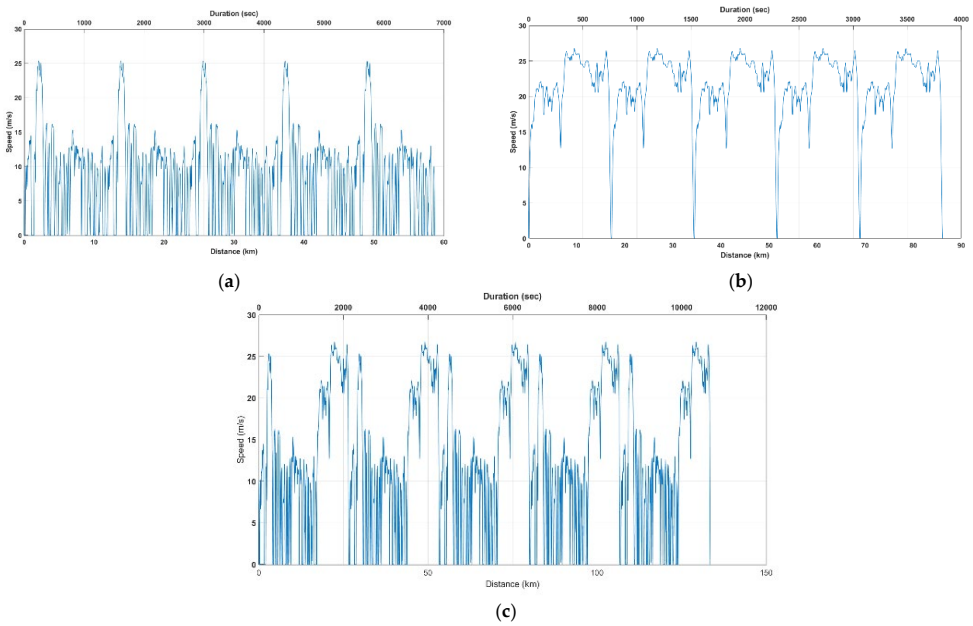

Figure 10. Drive traces: (**a**) UDDS (**b**) HWFET (**c**) UDDS-HWFET.

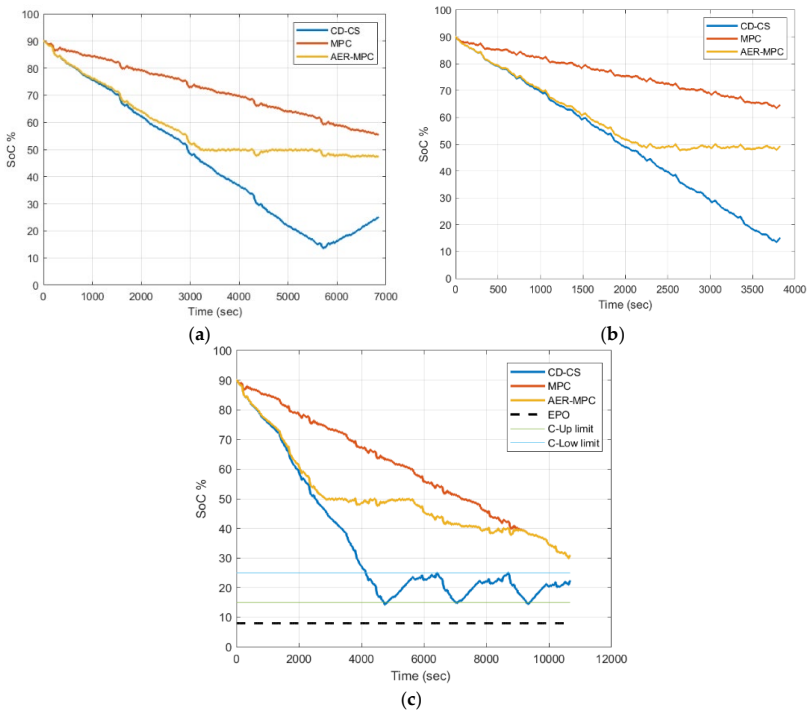

Figure 11. Actual SOC (**a**) UDDS (**b**) HWFET (**c**) UDDS-HWFET.

EPO (8%), C-Up (25%) and C-Low (15%) represent energy power off, upper and lower CS SOC limits, respectively. The optimal SOC trajectory obtained offline using DP is shown in Figure 12.

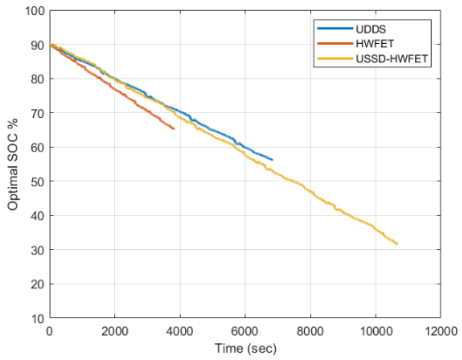

Figure 12. DP optimal SOC for the standard drive cycles.

3.2. Real-World Driving Cycle Results

Two drive traces were used: RM1 and RM2. To better evaluate the vehicle's performance, both drive traces were repeated several times. For RM1, it was repeated five times, and for RM2, it was repeated 15 times, but Figure 13b shows only six repetitions. The resulting total driving distance for RM1 and RM2 is equal to 117.68 km and 116.6 km, respectively. In addition, to simulate disturbances and uncertainties due to noise or inaccurate readings, random noise is added to the actual speed profile. The speed profile and simulation results are plotted in Figures 13 and 14, respectively.

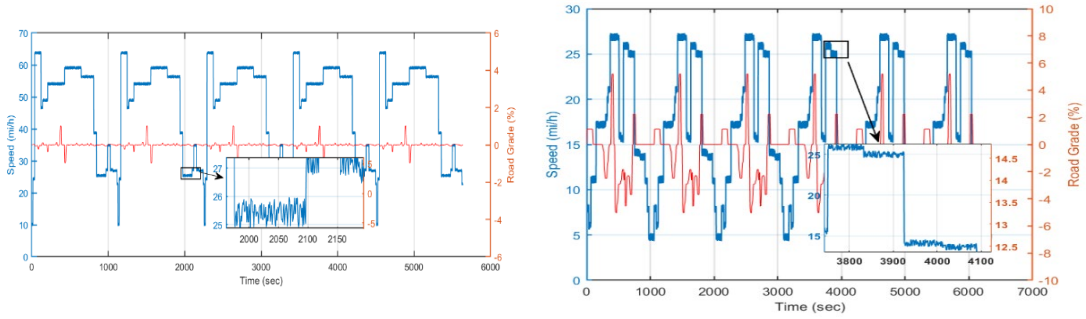

(**a**) (**b**)

Figure 13. Real drive traces: (**a**) RM1 (**b**) RM2.

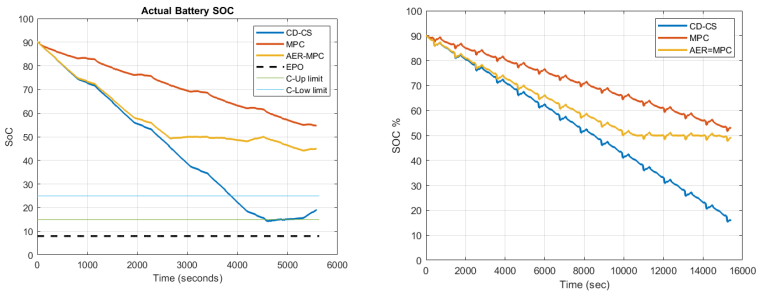

(**a**) (**b**)

Figure 14. Actual SOC: (**a**) RM1 (**b**)RM2.

The optimal SOC trajectory for the real-world drive cycles is shown in Figure 15. The EC for all drive traces is summarized in Table 4.

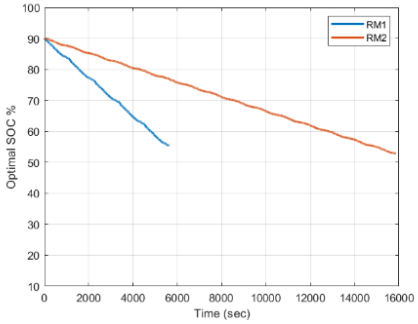

Figure 15. DP optimal SOC for real-world drive cycles.

Table 4. Control Strategies performance comparison.

Control Strategy	Energy Consumption kWh/km	EC Saving %
CD/CS: UDDS HWFET Combined	 0.206 0.171 0.222	 - - -
Traditional MPC: UDDS HWFET Combined	 0.135 0.094 0.089	 34.5 45 59
AER-MPC: UDDS HWFET Combined	 0.135 0.093 0.134	 34.5 45.6 39.6
CD/CS: RM1 RM2	 0.116 0.12	 - -
Traditional MPC: RM1 RM2	 0.06 0.067	 48.2 44
AER-MPC: RM1 RM2	 0.077 0.068	 33.6 43.3

When the vehicle operates as an EV, it utilizes only the ESS for its energy demands, while it uses both the ESS and the generator as an HEV. The use of the generator for the three strategies was evaluated for two drive traces, which are the combined drive cycle and RM1. The result is shown in Figure 16.

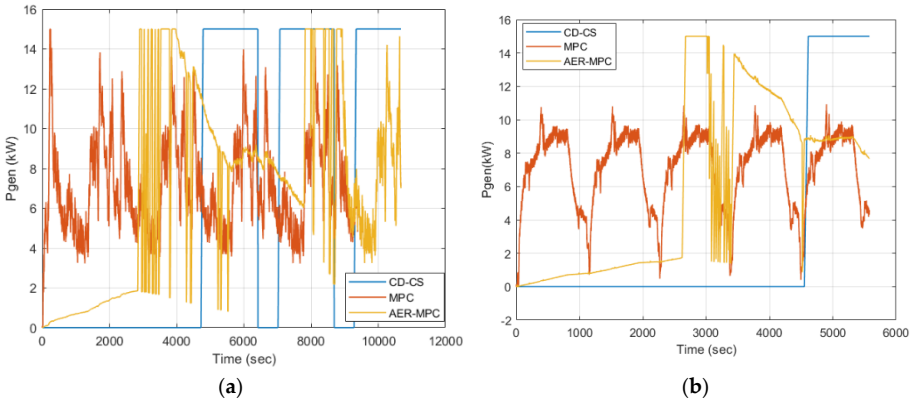

(**a**) (**b**)

Figure 16. Generator power usage: (**a**) Combined drive cycle (**b**) RM1 Drive.

4. Discussion

For the three standard drive cycles, all controllers' ESS SOCs decreased to a different final SOC. It can be seen to be lower as the travelled distance increases. For the MPC, the SOC decreases more slowly than the conventional CD/CS and AER-MPC since it prefers following the optimal SOC trajectory obtained using DP (Figures 12 and 15), but at the cost of extra fuel consumption by the generator (excess usage of fuel). On the other hand, a sharp drop in SOC is observed during CD for the CD/CS strategy till it reaches its minimum limit of about 15% when a CS mode is activated. This fast drop will cause less fuel consumption but a faster battery depletion (excess usage of ESS energy). The proposed controller follows the conventional algorithm until SOC reaches 50%; then, it prefers to follow the optimal path of SOC obtained using DP. From Figure 11, it can be concluded that the SOC in the case of HWFET speed profile depleted faster than the UDDS since it has a higher power demand.

Nevertheless, EC in the UDDS case is higher (longer driving distance). As in Table 4, the combined drive cycle has the highest EC among the three traces in the case of the conventional algorithm, but it is close to UDDS in our proposed AER_MPC. The energy saving for the proposed strategy shows satisfactory results, especially for the HWFET case.

For the real-world traces, it can be observed that RM1 has a relatively higher speed than RM2. As a result, it took much less time to reach the target distance (117.68 km). The final SOC for RM2 has barely reached the CS lower limit (15%) for the conventional strategy (Figure 14). From Table 4, it is evident that the EC value is lower in RM1 for the CD/CS strategy, but it is higher in RM1 for AER-MPC strategy. Generally, the energy-saving results using our algorithm were good for both traces. As seen from Table 4, EC savings for traditional MPC and AER-MPC are higher than the conventional CD/CS strategy. However, the SOC trajectory for the AER-MPC shows a better balance in terms of using the generator system more frequently and this leads to moderate use of the fuel among the other two strategies.

The generator power analysis in Figure 16 reveals that the MPC strategy uses the generator system frequently and in the same changing values along the travelled distance. In contrast, for CD/CS, the generator has worked later and much less regularly, and has two values (0 or 15 kW). For AER-MPC, the generator goes on earlier than CD/CS, and its value is adaptable and changes along the whole trace. Longer distance causes an increase in the generator run-time, which increases fuel usage to sustain ESS SOC.

5. Conclusions

This study presents an energy management strategy that minimizes energy consumption for hybrid electric vehicles and prevents battery SOC from dropping quickly to its critical threshold level. A conventional energy management controller prefers to use ESS to reduce fuel consumption. However, this may cause a severe depletion of the ESS SOC and, consequently, a reduction of the life of the battery. So, there is a trade-off between two objectives: battery energy consumption and fuel consumption. The ARE-MPC algorithm tried to balance between these two objectives. It revealed that the generator system had been activated earlier to sustain SOC, then it prefers to follow optimal SOC obtained offline using DP. The EC comparison for several speed profiles demonstrates that our suggested algorithm outperforms both the original MPC and conventional algorithms.

There are several challenges when moving from implementing an energy management strategy for an HEV initially developed and tested in a simulation of real-world implementation; for example, the cost, integration with complex control units that support MPC-based EMS, and extensive HIL testing to validate its performance under realistic operating conditions (this can be considered a suggestion for future work). Possible limitations include sensor accuracy, significant computational power to solve optimization problems in real-time, and unpredictable driving conditions, such as aggressive driving, or extreme weather conditions. By addressing these challenges and limitations, the proposed strategy

can successfully transition from simulation to a real HEV, optimizing energy usage while ensuring safe and efficient vehicle operation.

Finally, the suggested algorithm would suit EREVs and series HEVs but it would need a certain modification to handle the complexity of the other hybrid vehicle architectures such as parallel or series-parallel HEVs.

Author Contributions: Methodology, F.M.A.; investigation, F.M.A.; data curation, F.M.A.; writing—original draft preparation, F.M.A.; formal analysis, F.M.A. and N.H.A.; review and editing, N.H.A.; supervision, N.H.A.; project administration, N.H.A. All authors have read and agreed to the published version of the manuscript.

Funding: This research received no external funding.

Data Availability Statement: The data can be provided upon request.

Acknowledgments: This work was supported by the Electrical Engineering Department, College of Engineering, University of Baghdad under Grant No. 18211.

Conflicts of Interest: The authors declare no conflict of interest.

References

1. Li, L.; Zhang, Y.; Yang, C.; Yan, B.; Martinez, C. Model Predictive Control-based Efficient Energy Recovery Control Strategy for Regenerative Braking System of Hybrid Electric Bus. *Energy Convers. Manag.* **2016**, *111*, 299–314. [CrossRef]
2. Millo, F.; Rolando, L.; Tresca, L.; Pulvirenti, L. Development of a Neural Network-based Energy Management System for a Plug-in Hybrid Electric Vehicle. *Transp. Eng.* **2023**, *11*, 100156. [CrossRef]
3. Tran, D.; Vafaeipour, M.; El Baghdadi, M.; Barrero, R.; Mierlo, J.; Hegazy, O. Thorough State-of-the-art Analysis of Electric and Hybrid Vehicle Powertrains: Topologies and Integrated Energy Management Strategie. *Renew. Sustain. Energy Rev.* **2020**, *119*, 109596. [CrossRef]
4. Zhao, Z.; Xun, J.; Wan, X.; Yu, R. MPC Based Hybrid Electric Vehicles Energy Management Strategy. *IFAC-PapersOnLine* **2021**, *54*, 370–375. [CrossRef]
5. Wang, Y.; Jiao, X. Dual Heuristic Dynamic Programming Based Energy Management Control for Hybrid Electric Vehicles. *Energies* **2022**, *15*, 3235. [CrossRef]
6. Qi, C.; Zhu, Y.; Song, C.; Yan, G.; Xiao, F.; Wang, D.; Zhang, X.; Cao, J.; Song, S. Hierarchical Reinforcement Learning Based Energy Management Strategy for Hybrid Electric Vehicle. *Energy* **2022**, *238*, 121703. [CrossRef]
7. Hofman, T.; Steinbuch, M.; van Druten, R.M.; Serrarens, A.F.A. Rule-based Energy Management Strategies for Hybrid Vehicle Drivetrains: A Fundamental Approach in Reducing Computation Time. *IFAC* **2006**, *39*, 740–745. [CrossRef]
8. Bagwe, R.M.; Byerly, A.; Santos, E.C.D.; Ben-Miled, Z. Adaptive Rule-Based Energy Management Strategy for a Parallel HEV. *Energies* **2019**, *12*, 4472. [CrossRef]
9. Taghavipour, A.; Moghadasi, S. A Real-Time Nonlinear CRPE Predictive PHEV Energy Management System Design and HIL Evaluation. *IEEE Trans. Veh. Technol.* **2021**, *70*, 49–58. [CrossRef]
10. Vinot, E.; Trigui, R. Optimal Energy Management of HEVs with Hybrid Storage System. *Energy Convers. Manag.* **2013**, *76*, 437–452. [CrossRef]
11. Jegede, T.; Knowles, J.; Steffen, T.; D'Amato, M.; Maganga, O. *Evaluation of Optimal State of Charge Planning Using MPC*; SAE International: Warrendale, PA, USA, 2022. [CrossRef]
12. Jiang, Q.; Ossart, F.; Marchand, C. Comparative Study of Real-Time HEV Energy Management Strategies. *IEEE Trans. Veh. Technol.* **2017**, *66*, 10875–10888. [CrossRef]
13. Xie, S.; Hu, X.; Xin, Z.; Brighton, J. Pontryagin's Minimum Principle based Model Predictive Control of Energy Management for a Plug-in Hybrid Electric Bus. *Appl. Energy* **2019**, *236*, 893–905. [CrossRef]
14. Vadamalu, R.S.; Buch, D.; Xiao, H.; Beidl, C. Energy management of Hybrid Electric Powertrain using Predictive Trajectory Planning Based on Direct Optimal Control. *IFAC-PapersOnLine* **2015**, *48*, 236–241. [CrossRef]
15. Schwenzer, M.; Muzaffer, A.; Bergs, T.; Abel, D. Review on Model Predictive Control: An Engineering Perspective. *Int. J. Adv. Manuf. Technol.* **2021**, *117*, 1327–1349. [CrossRef]
16. He, H.; Wang, Y.; Han, R.; Han, M.; Bai, Y.; Liu, Q. An Improved MPC-based Energy Management Strategy for Hybrid Vehicles using V2V and V2I Communications. *Energy* **2021**, *225*, 120273. [CrossRef]
17. Wang, W.; Guo, X.; Yang, C.; Zhang, Y.; Zhao, Y.; Huang, D.; Xiang, C. A multi-objective Optimisation Energy Management Strategy for Power Split HEV Based on Velocity Prediction. *Energy* **2022**, *238*, 121714. [CrossRef]
18. East, S.; Cannon, M. Energy Management in Plug-In Hybrid Electric Vehicles: Convex Optimization Algorithms for Model Predictive Control. *arXiv* **2019**, arXiv:1902.07728v2. [CrossRef]
19. Chen, H.; Xiong, R.; Lin, C.; Shen, W. Model Predictive Control Based Real-time Energy Management for Hybrid Energy Storage System. *CSEE J. Power Energy Syst.* **2021**, *7*, 862–874.

20. Lin, B.; Wei, C.; Feng, F.; Liu, T. A Predictive Energy Management Strategy for Heavy Hybrid Electric Vehicles Based on Adaptive Network-Based Fuzzy Inference System-Optimized Time Horizon. *Energies* **2024**, *17*, 2288. [CrossRef]
21. Chen, Z.; Hu, H.; Wu, Y.; Zhang, Y.; Li, G.; Liu, Y. Stochastic model predictive control for energy management of power-split plug-in hybrid electric vehicles based on reinforcement learning. *Energy* **2020**, *211*, 118931. [CrossRef]
22. Wahid, M.R.; Budiman, B.A.; Joelianto, E.; Aziz, M. A Review on Drive Train Technologies for Passenger Electric Vehicles. *Energies* **2021**, *14*, 6742. [CrossRef]
23. Kalia, A.V.; Fabien, B.C. On Implementing Optimal Energy Management for EREV Using Distance Constrained Adaptive Real-Time Dynamic Programming. *Electronics* **2020**, *9*, 228. [CrossRef]
24. Lin, W.; Zhao, H.; Zhang, B.; Wang, Y.; Xiao, Y.; Xu, K.; Zhao, R. Predictive Energy Management Strategy for Range-Extended Electric Vehicles Based on ITS Information and Start–stop Optimisation with Vehicle Velocity Forecast. *Energies* **2022**, *15*, 7774. [CrossRef]
25. Xiao, B.; Ruan, J.; Yang, W.; Walker, P.D.; Zhang, N. A review of Pivotal Energy Management Strategies for Extended Range Electric Vehicles. *Renew. Sustain. Energy Rev.* **2021**, *149*, 111194. [CrossRef]
26. Musardo, C.; Rizzoni, G.; Guezennec, Y.; Staccia, B. A-ECMS: An Adaptive Algorithm for Hybrid Electric Vehicle Energy Management. *Eur. J. Control* **2005**, *11*, 509–524. [CrossRef]
27. Gillespie, T.D. *Fundamentals of Vehicle Dynamics*, Revised ed.; SAE International: Warrendale, PA, USA, 2021.
28. Tremblay, O.; Dessaint, L.A. Experimental Validation of a Battery Dynamic Model for EV Applications. *World Electr. Veh. J.* **2009**, *3*, 289–298. [CrossRef]
29. Wehbe, J.; Karami, N. Battery Equivalent Circuits and Brief Summary of Components Value Determination of Lithium Ion: A review. In Proceedings of the Third International Conference on Technological Advances in Electrical, Electronics and Computer Engineering, Beirut, Lebanon, 29 April–1 May 2015; pp. 45–49.
30. Prasanthi, A.; Shareef, H.; Asna, M.; Ibrahim, A.A.; Errouissi, R. Optimisation of Hybrid Energy Systems and Adaptive Energy Management for Hybrid Electric Vehicles. *Energy Convers. Manag.* **2021**, *243*, 114357. [CrossRef]